Sensors & Transducers Journal, Vol. 137, Issue 2, February 2012, pp. 22-35

www.sensorsportal.com

Sensors & Transducers

ISSN 1726-5479

http://www.sensorsportal.com

Mechanistic Modeling, Simulation and Control of Humidity Sensor Characteristics

Vinod Kumar KHANNA

MEMS & Microsensors, Solid-State Devices Division, CSIR-Central Electronics Engineering Research Institute, Pilani-333031 (Rajasthan), India

Tel.: +91-1596-252353, fax: +91-1596-242294

E-mail: vkk_ceeri@yahoo.com

Received: 29 November 2011 /Accepted: 14 February 2012 /Published: 28 February 2012

Abstract: Humidity sensors are required for diverse applications in low and high humidity ranges. Also, fast-response humidity sensors are sometimes needed. For this purpose, it is necessary to understand the hygroscopic influences and physico-chemical mechanisms underlying sensor operation as well as their correlation with the terminal properties of sensors. Several models and theories of sensors have been proposed for interpretation of their behaviour. This paper comprehensively surveys the available models and points out the utilization of selected models for tailoring sensor characteristics in accordance with intended application. Ionic salt doping is a useful technique for improving the sensitivity, linearity and hysteresis of humidity sensor characteristics.

Keywords: Humidity sensor, Capacitor, Modeling, Simulation, Physico-chemical mechanisms.

1. Introduction

Solid-state sensors hold the key to the application of microelectronics in several areas such as analytical instruments, pharmaceuticals, deliquescent chemicals, photography, product drying (tea, coffee, sugar, etc.), and myriad other applications. The 'humidity sensor' is the heart of all humidity measurement and monitoring instrumentation. A small, easy-to-use, reliable, high sensitivity, low cost humidity-sensing device is any instrument designer's favourite. Especially, micro humidity sensors have aroused considerable interest during the last few decades. Impetus for this development has been provided by the rapid strides made by integrated circuit technology and widespread use of microprocessor-based instrumentation, resulting in the exploration of new structures and a renewed quest for sensing materials.

Constructionally, a humidity sensor consists of either: (i) a porous dielectric film of anodic aluminium oxide or polyimide/humidity-sensitive polymer or ceramic material sandwiched between two conducting electrodes, or (ii) a porous dielectric film of any of the above materials overlaid with an interdigitated pair of metal electrodes. The variation of capacitance or resistance of the structure with moisture content is exploited for humidity sensing. Accordingly, the sensor is referred to as a capacitive or resistive humidity sensor [5-14]. These two basic classes have been the primary or pivotal devices in the burgeoning domain of humidity sensors.

Two vital properties of a humidity sensor are *sensitivity* defined as the change in capacitance per unit % relative humidity change and *response time*, the time taken by the sensor to respond to a sudden or step change in humidity. Obviously, for fabrication of a humidity sensor with desired response characteristics, it is essential to understand the physical origin of its humidity-sensing behaviour. Also, one must know the interrelation of genesis of this behaviour with the growth or deposition conditions of the dielectric film used in the device. The geometrical layout of the top metal electrode also plays a significant role in sensor response. For explaining the properties of humidity sensors, models have been developed sporadically and presented by researchers from time to time. Unfortunately, attempts to describe the characteristics in terms of physical and chemical processes have received little attention, despite the fact that several publications have appeared on various types of humidity sensors, including those using MEMS technologies [15-16] and nanomaterials [17-21]. As the basic processes controlling sensor behaviour have scarcely been addressed, it is necessary to review them for acquisition of a better perspective of humidity sensor scenario. The motivation for re-examination of humidity sensor models lies in the valuable practical insights provided by them regarding the controlling parameters that one needs to consider for fabrication of sensors as per performance expectations. The novel ideas generated by this analysis also help in paving the pathway towards improvement in performance characteristics and realizing the limitations of the sensors. Particularly, mechanistic modeling is concerned with description of sensor properties in terms of rudimentary physico-chemical phenomena and mechanisms governing the sensor operation

The mechanistic models for humidity sensors in the literature are categorized into two main heads, viz., equivalent circuit models and those based on dielectric theories of porous solids. The present paper outlines the prominent models of both categories, and brings out their utility for understanding sensor properties as well as for designing humidity sensors with specified features. Interesting humidity sensing structures that have been developed and modeled, have also been outlined. This paper is organized as follows: Sec. 2 describes equivalent circuit models. Sec. 3 is devoted to theory of humidity sensor founded on Sillars' dielectric formulation. In Secs. 4-6, the analysis of innovative example cases of humidity sensor structures for fast response is presented. Sec. 7 critically assesses the models and suggests design guidelines for these sensors. Sec.8 summarizes the contemporary issues and sketches future perspectives.

2. Equivalent Circuit Models of Humidity Sensors

An epoch-making model is that of Jason, Wood and others [22-24] which they framed for interpreting the electrical characteristics of porous alumina humidity sensor developed by them (Fig. 1). The model replaces the sensor by an equivalent circuit consisting of passive components: resistors and capacitors. In this circuit, C_0, R_0 represent the capacitance and resistance of (solid Al_2O_3 + air + water) system; C_B, R_B denote the same for pore base; and R_S is the variable pore side or pore wall resistance which alters with humidity. Changes in the values of R_S with humidity were used to qualitatively account for the observed properties of the sensor but a quantitative calculation of the sensor parameters at different humidities or its frequency-dependent response could not be provided.

Quantitative modeling was later attempted by Nahar and Khanna [7] based on Maxwell-Wagner effect and Falk et al. [25] through a nonlinear curve fitting procedure. However, a humidity sensor is a complex device, and substitution of the sensor by a simplified equivalent circuit fails to provide a satisfactory explanation of sensor properties leaving too many unresolved questions and gaps in knowledge.

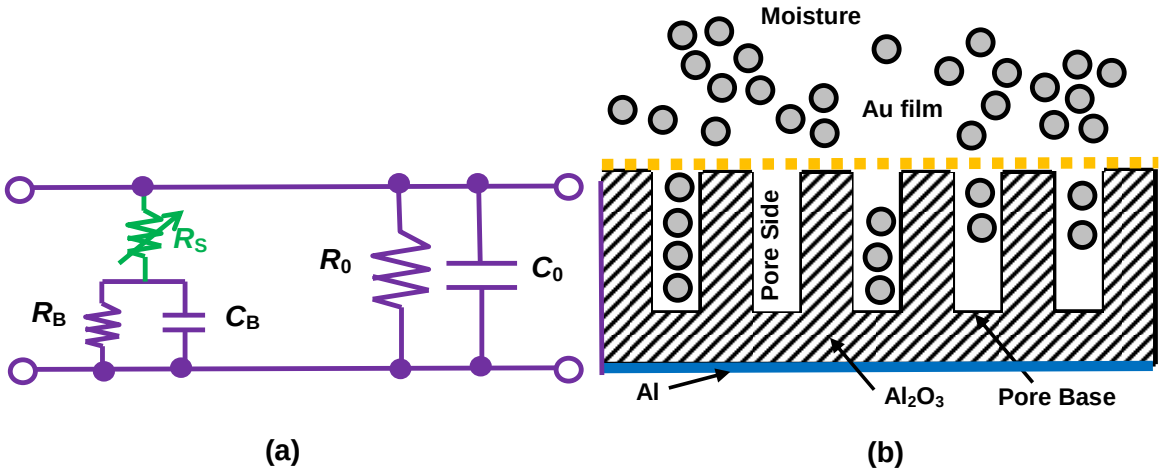

Fig. 1. (a) Jason-Wood equivalent circuit of Al_2O_3 humidity sensor; (b) Au-Al_2O_3–Al structure of the sensor.

3. Theory of Al_2O_3 Humidity Sensor Based on Dielectric Properties of Porous Solids

In a series of papers, Khanna, Nahar and others [26-33] proposed a theory of the sensor based on: (i) The established picture of adsorption of water on a metal oxide in which, first a layer of water is chemisorbed on the sensor surface leading to hydroxylation of the entire surface. Subsequent layers of water condense by physisorption on the bottom chemisorbed layer. (ii) *Brunauer-Emmett-Teller (BET) theory of adsorption*: in which physisorption takes place by building up a monomolecular layer of water on the whole hydroxylated surface of the sensor, and then further layers of water are adsorbed in sequence, i.e., the second, third, … layers, each successively on the layer underneath it, to form multilayers. This adsorption follows the familiar BET equation [34-35]. Capillary condensation of moisture occurs at high humidities when the diameters of the pores satisfy Kelvin's equation [36]. (iii) Up to the completion of the first layer of water, the adsorbed water film is discontinuous and electrical conduction takes place by electron tunneling between neighbouring water sites which donate electrons to the alumina surface (Fig. 2). After the first layer is completed by coalescence of adjacent water islands formed on the sensor surface, bulk water properties are postulated and protonic conduction occurs, as in an electrolyte. (iv) The adsorbed water in the porous film constitutes a dielectric system incorporating semiconducting particles (in the form of water molecules) suspended in an insulating matrix. Both the shape of this inclusion and the conductivity of water are decisive when calculating the properties of this composite dielectric. It is amenable to Sillars' formalism propounded in 1937 [37]. (v) As the porous anodic aluminium oxide film exhibits a normal distribution of pore diameters on its surface, anion incorporation into the film during its growth also complies with this distribution function. Further, because the conductivity due to tunneling mechanism at low humidities varies as the logarithm of the distance between the ions and also the electrolytic conductivity, by Debye-Huckel theory [38], is inversely proportional to logarithm of ionic concentration, it is evident that logarithm of surface conductivity obeys normal distribution function, so that a *log-normal distribution of surface conductivity* amongst the pores, irresistibly follows. Anion doping assists electronic transport at low humidities by providing additional sites between which tunneling can occur. But it degrades the higher humidity sensitivity by lowering the surface conductivity via increase in electrolytic concentration.

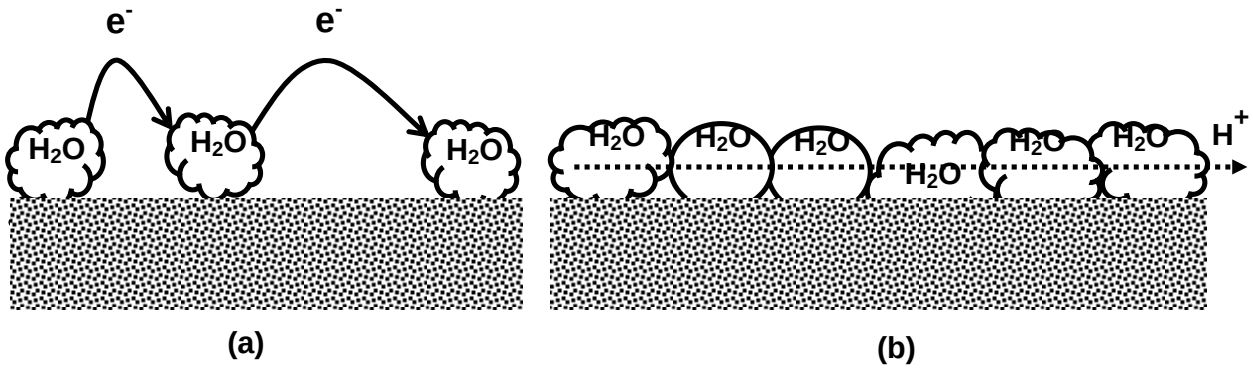

Fig. 2. Electrical transport mechanisms on sensor surface: (a) Electron tunneling between separate adsorbed water sites, and (b) Liquid-like conduction in continuous water film.

The moisture-sensitive capacitance of the sensor is described in terms of the real component ε' of a complex dielectric constant given by [26]

$$\varepsilon' = \varepsilon_{\mathrm{m}} + \frac{\varepsilon_{\mathrm{m}}\,\Gamma}{1+\omega^2\tau^2}, \tag{1}$$

where ϵ_{m} is the relative permittivity of solid-air mixture, Γ is a parameter related shape of the pores, ω is the frequency of operation and τ is the time constant.

Applying this theory, the equations derived for low and high humidity cases were used for theoretically computing the capacitance-humidity characteristic of an Al_2O_3 sensor at a specified current density J_2, utilizing a given experimental characteristic of the sensor fabricated at a different current density J_1. At low levels of humidity η [31], the ratio of resulting humidity sensitivities $(d\varepsilon'/d\eta)_1/(d\varepsilon'/d\eta)_2$ is

$$\left(d\varepsilon'/d\eta\right)_1 \Big/ \left(d\varepsilon'/d\eta\right)_2 = \exp\left\{\xi \ln\left(J_2/J_1\right)\right\}\exp\left\{-4\left(1/J_2 - 1/J_1\right)\right\}, \tag{2}$$

where ξ, ξ' are constants with typical values: $\xi = 0.32$, $\xi' = 0.20$. At high humidities η, the sensitivity ratio becomes [31]

$$\left(d\varepsilon'/d\eta\right)_1 \Big/ \left(d\varepsilon'/d\eta\right)_2 = \exp\left\{\xi \ln\left(J_2/J_1\right)\right\}\exp\left\{-4\left(\sqrt{J_2} - \sqrt{J_1}\right)\right\}, \tag{3}$$

The simulated characteristics of Al_2O_3 sensors fabricated at different anodization current densities are shown in Fig. 3, which demonstrates the utility of this model for fabricating sensors for different humidity ranges because the sensor fabricated at 1 mA cm^{-2} current density is more sensitive at high humidities while that made with Al_2O_3 film grown at 10 or 20 mA cm^{-2} is superior at low humidities [31].

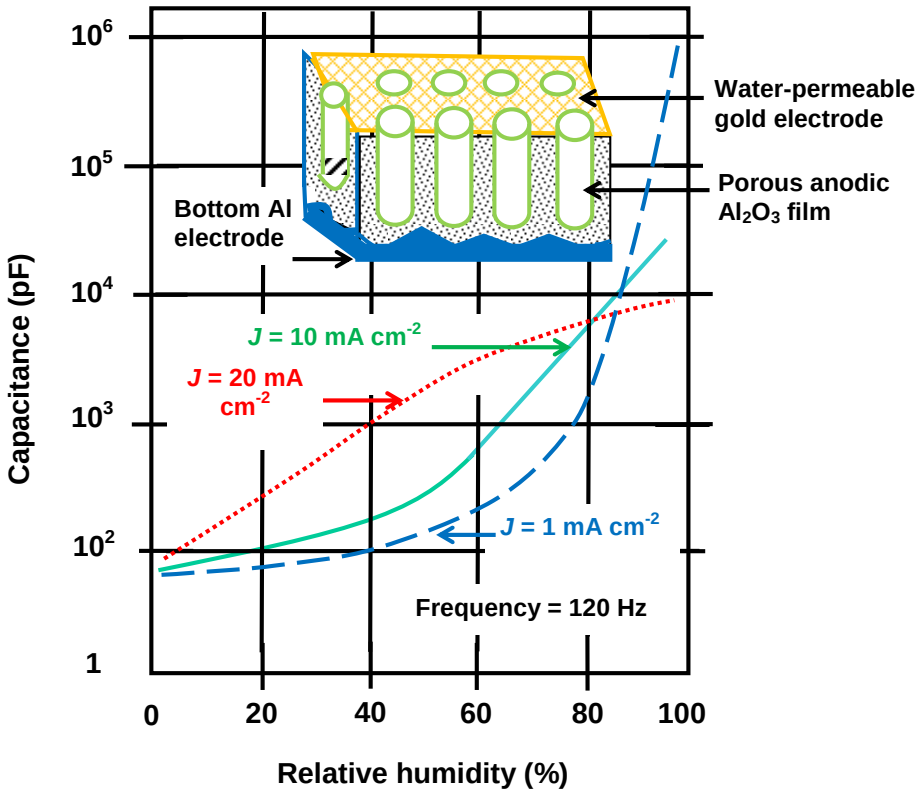

Fig. 3. Inversion of humidity sensor characteristics according to the simulations of Nahar and Khanna [31]. Capacitance characteristics of a thin film Au-porous anodic Al_2O_3-Al capacitive humidity sensor at different current densities are simulated taking experimental J= 10 mAcm^{-2} curve as a reference. Inset shows the cross-section of this moisture sensor.

4. Fast Humidity-Sensing Structure and its Modeling

Kang and Wise [39] argued that for fabrication of a quick-response humidity sensor, there are two possibilities: either one should use an insulating material with a large diffusion coefficient for water vapour, or modify the basic configuration of the sensor. They came up with a novel configuration comprising vertical polyimide columns arranged below an electrode array so that moisture could penetrate the insulator from the top downwards as well as in the lateral or sideways direction, i.e., all around the circumference. The sensor also had an on-chip thermal reset for speedy recovery.

Fig. 4 makes a comparison of sensor structures offering water penetration from top downwards with lateral diffusion, and with inclusion of circumferential adsorption.

The structure adopted by Kang and Wise [39] is depicted in Fig. 5(a) while Fig. 5(b) displays the dynamic response of water adsorption by a simple thin film and a cylindrical structure. The formulation of these workers is framed as follows: For diffusion in a film, the capacitance after normalization with respect to the final capacitance, is [39]

$$C_{\text{Norm,Film}}(t) = \sum_{n=1}^{\infty} \frac{1-\exp\dfrac{-(2n-1)^2\pi^2 Dt}{4h^2}}{(2n-1)^2} \Bigg/ \sum_{n=1}^{\infty} \frac{1}{(2n-1)^2}, \tag{4}$$

where n is an integer, D is the diffusion constant of moisture, h is the height of the film and t is the time.

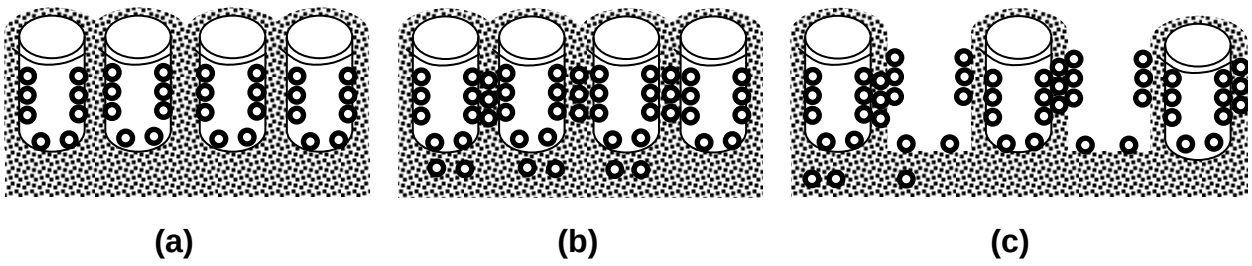

Fig. 4. (a) Adsorption of water vapour on pore walls, (b) Adsorption followed by lateral diffusion into pore walls and bottom, (c) Adsorption into pore walls, lateral diffusion and circumferential adsorption.

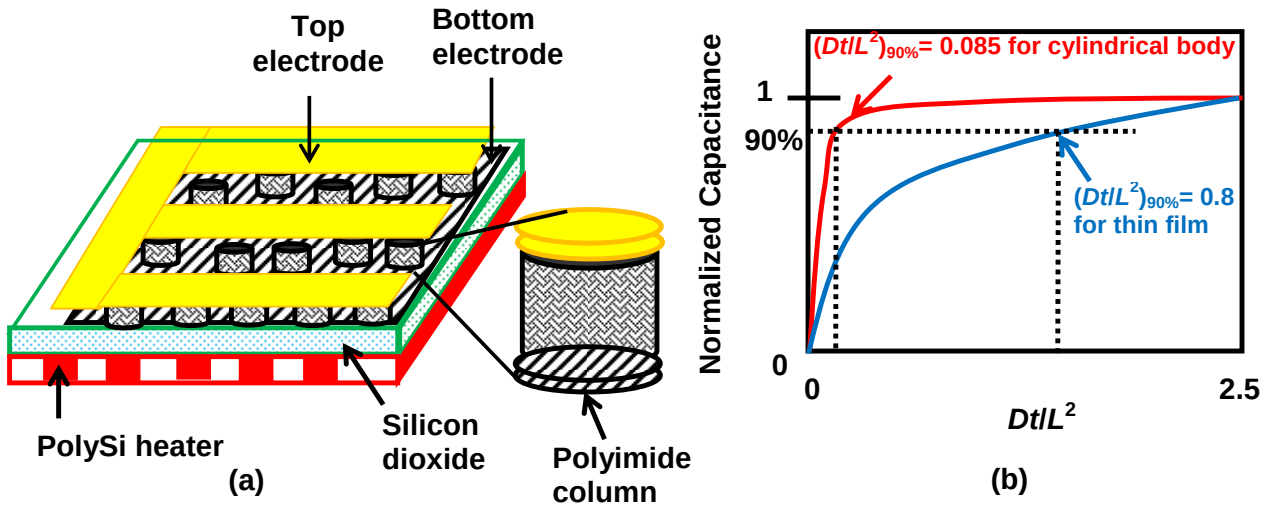

Fig. 5. Concept of circumferential, top-down and lateral moisture adsorption utilized in high-speed capacitive humidity sensor with on-chip thermal reset: (a) Constructional diagram showing polyimide columns and integrated heater; the supporting substrate is Si_3N_4-Si (not shown). (b) Typical simulated responses for step humidity change for thin film and cylindrical structures from the model of Kang and Wise [39].

As the normalized capacitance is proportional to Dt/h^2, it is evident that the response time

$$t_{\text{Film}} \propto 1/D \quad \text{and} \quad t \propto h^2 \tag{5}$$

For diffusion into a cylindrical body with radius a of the base [39],

$$C_{\text{Norm,Cyl}}(t) = \sum_{n=1}^{\infty} \frac{1-\exp\left(-Dk_n^2 t/a^2\right)}{k_n^2} \Big/ \sum_{n=1}^{\infty} \frac{1}{k_n^2}, \tag{6}$$

where k_n's are the roots of the equation

$$J_0(k) = 0\,, \tag{7}$$

J_0 is the Bessel function of the first kind of zero order.

Because the normalized capacitance is proportional to Dt/a^2, it is clear that the response time

$$t_{\text{Cyl}} \propto 1/D \quad \text{and} \quad t \propto a^2 \tag{8}$$

Applying equations (4) and (6), from analytically calculated response times for diffusion into a thin film and into a cylindrical body, Kang and Wise observed that for a step humidity change, it will take a time interval = 0.85 h^2/D for the film and = 0.08 h^2/D for the cylindrical body to attain 90 % value of the eventual capacitance under equilibrium condition. This gives a ten-fold improvement in response time for lateral diffusion-based device [39].

5. Dynamic Response Analysis of a Humidity Sensor with a Top Grid Electrode

Tetelin and Pellet [40-42] mathematically modeled the transient response of a humidity sensor with a top electrode made of parallel fingers. They performed the analysis as a function of width of the fingers and the inter-finger spacing. In this structure, moisture propagates downwards and also laterally in a polymer layer (Fig. 6); there is no circumferential adsorption. They applied Henry's and Fick's laws to predict the transient response of the sensor. The adsorption stage is governed by Henry's law and the diffusion stage by Fick's law. The impulse response of the sensor is expressed as [40]

$$h_{\mathbf{Q}}(t) = lpq \times \frac{2D}{d} \sum_{n=1}^{\infty} \exp\left\{\frac{-D(2n-1)\pi^2 t}{4d^2}\right\} + ldq \times \frac{4D}{r} \sum_{n=1}^{\infty} \exp\left\{\frac{-D(2n-1)\pi^2 t}{r^2}\right\}, \tag{9}$$

where D is the diffusion coefficient or diffusivity in the Henry mode, t is the time, l is length of the film, p is interline spacing, q is the number of lines, r is width of the line, and d is the thickness of the film. Simulation carried out for n= 1 up to50, provided sufficient accuracy.

6. Numerical Modeling of Capacitive Humidity Sensor

Chandran et al. [43] performed 3-D modeling of integrated capacitive humidity sensors based on interdigitated microelectrodes coated with a moisture-absorbing dielectric. By solving the Laplace equation using appropriate boundary conditions, they found the electric potential and field distributions outside the electrodes. The solution also determined the surface charge induced on the electrodes, which helped in obtaining the capacitance of the complete structure.

Sen and Zarabi [44] proposed a finite-element model of a capacitive humidity sensor (Fig. 7). Parallel and interdigitated Au/Cr top and bottom electrodes were used with a polyimide sensing layer. The top electrode had holes for moisture adsorption into the solid.

Poisson's equation was solved for computing the electric field in the computational domain:

$$-\nabla \cdot (\varepsilon_0 \varepsilon_s \nabla V) = \rho \tag{10}$$

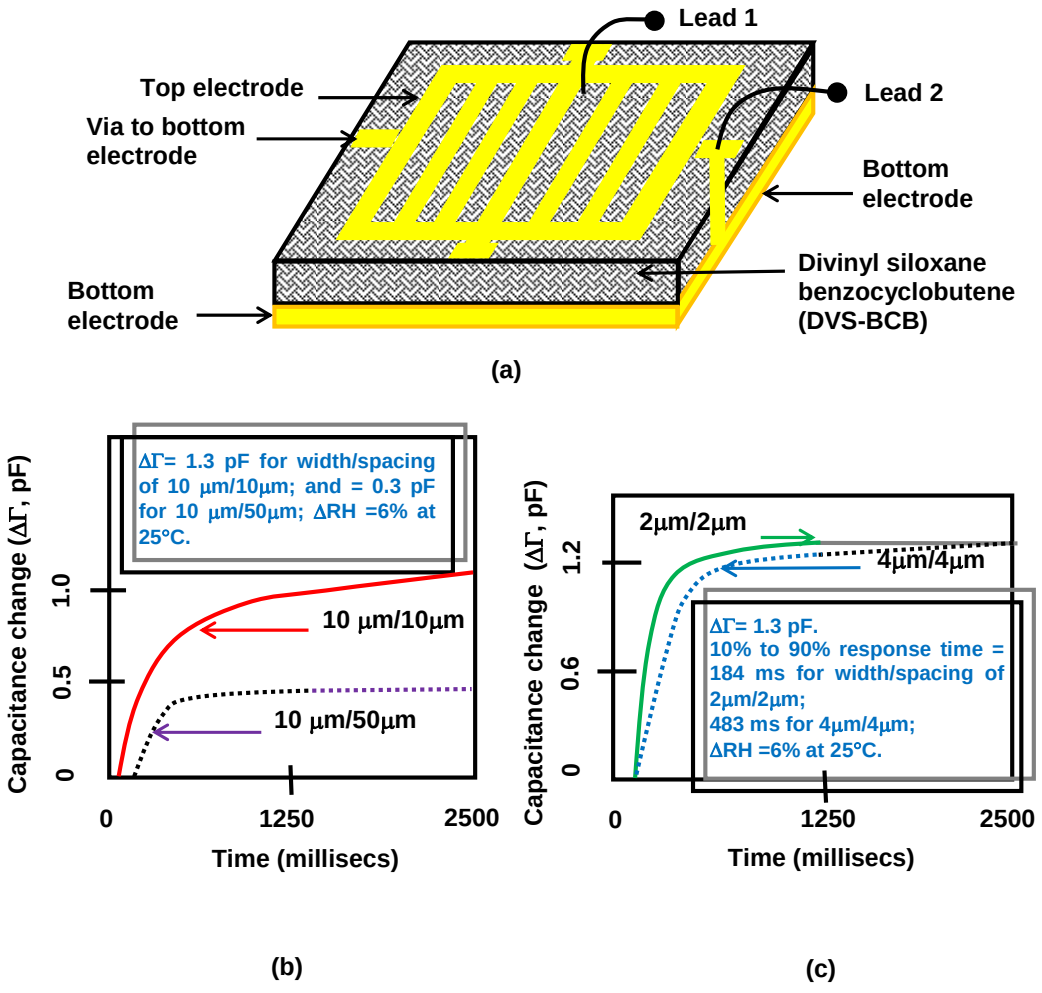

Fig. 6. Effect of finger widths/spacings on the transient response of a polymer humidity sensor: (a) Schematic diagram showing the constituent layers in the sensor; the sensor is fabricated on SiO_2-Si substrate (not shown); (b) and (c): Representative simulation results of the model proposed by Tetelin and Pellet [40-42] for (b) dissimilar widths and spacings, and (c) similar width and spacing of fingers. The controlling principle is the downwards and lateral diffusion of moisture from the top surface.

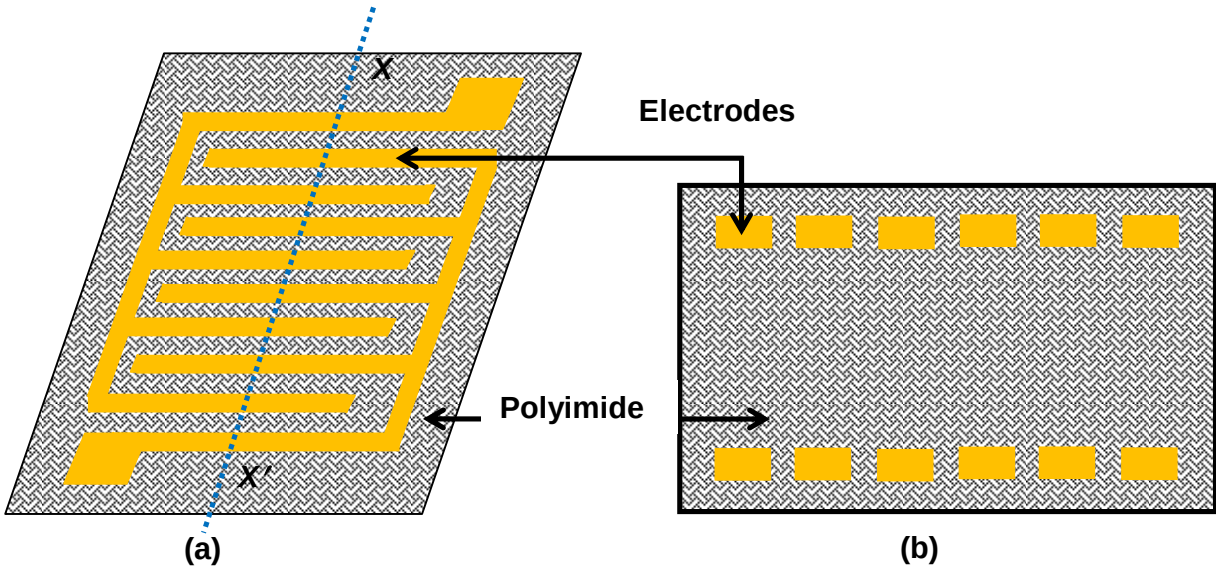

Fig. 7. (a) Top picture, and (b) cross-sectional view of the sensor (across *X*-*X′* plane) [34].

In this equation, V denotes the applied voltage across the sensing layer; ϵ_0, ϵ_s are free-space permittivity and relative permittivity of sensing film respectively; ρ is the density of space charge. The capacitance is found by calculating the electrical energy across the film. The model calculates the capacitance variation across the sensing layer with respect to relative humidity. The solution was independent of the number of cells when it was > 90, 000. The moisture content dependence on relative humidity is included through Looyenga's empirical model and that of Shibata eta al [45-47]:

$$\epsilon_s = \left\{\gamma\left(\epsilon_w^{1/3} - \epsilon_p^{1/3}\right) + \epsilon_p^{1/3}\right\}^3, \tag{11}$$

where γ is the volume fraction of water, ϵ_p is the dielectric constant of the sensing film without water and ϵ_w the dielectric constant of water, which at temperature T is given by

$$\epsilon_w = 78.54\left\{1 - 4.6 \times 10^{-4}(T - 298) + 8.8 \times 10^{-6}(T - 298)^2\right\} \tag{12}$$

They investigated the effect of metal electrode thickness on device sensitivity, and found that the sensitivity increased with thickness up to 0.8 μm. The reason suggested by them was that for the same sensing layer thickness, the electrode thickness increased the capacitance between a pair of top–bottom and adjacent electrodes. Improved transient response was also achieved at higher electrode thickness. Again, this was because the increase in the thickness of the electrodes increased the capacitance between two adjacent electrodes, located at the upper portion of the sensing layer. Furthermore, it was found that the sensitivity was highest for the situation in which the electrode width = 2 × electrode gap, which was ascribed to increased capacitance due to larger electrode area.

7. Discussions

The survey of humidity sensor literature showed that sensor technology has been the target of intensive research and development endeavors, and a wide spectrum of sensors has emerged. On the contrary and quite surprisingly too, the physical understanding of sensor properties has evoked little interest. Insufficient efforts have been made to interpret the experimental humidity sensor characteristics in terms of device physics. Papers on humidity sensors contained only a few sentences of a rather general description on the physical mechanisms. This did not provide the desired understanding.

Delving into the humidity sensor models, one finds that no single model is able to represent the multiplicity of phenomena that account for the observed properties of the humidity sensor. Indeed, the humidity sensor output is an intermixture of intricate processes taking place simultaneously and in tandem. The equivalent circuit model offers a simplified picture of the sensor without mathematical complexity but does not afford deterministic analysis. Studying sensor properties on the premise of Sillars' formalism is fairly complete in so far as the dielectric properties are concerned because it incorporates the effects of pore shapes and surface conductivity variations from pore to pore as well as with humidity. However, diffusion of moisture into the pore walls is not mathematically included in this model. Therefore, it does not permit transient analysis, which is better represented by the models that take the diffusion of water vapour into consideration. Finite element analysis is accurate. Nonetheless, the formulae used to represent water vapour adsorption and the effective dielectric constant of solid containing moisture has limitations. The effect of temperature on the dielectric constant of water was included. But the effects of temperature on sensor properties is important and its satisfactory representation in all the parameters that together work together to determine sensor properties remains a challenge. Consideration of a large number of physico-chemical processes adds to mathematical complexity. Thus, taken as a whole, the picture is not represented by a single model. Depending on the application, a particular model may be selected that deals with the issues at hand, and its limitations properly understood. Then only realistic inferences can be drawn from it.

Regarding the information provided by models for sensor fabrication, process tuning and structural design, the following remarks are made: Choice of suitable material for sensor fabrication is the starting step. The key to fabricating humidity sensors for low and high humidities lies in ionic doping of the sensor surface. Anionic doping is an inherent consequence of anodic growth. Anion incorporation into porous anodic Al_2O_3 film is controlled through anodization current density during film growth. The anions introduced from the electrolyte into the oxide exert a strong influence on the physical and chemical properties of the film, viz., electronic and ionic surface conductivities. A significant quantity of anions enter the films grown in sulphuric acid while in other electrolytes, the proportion is comparatively low. In films formed in chromic acid, 0.4-0.7 % chromic acid is detected compared with 3 % oxalate and 10-17 % SO_4^{2-} ion uptake in films formed in oxalic and sulphuric acids respectively [48]. This may be related to the ease of anion adsorption on the surface, sulphate ion adsorption being easier than chromate, dichromate or oxalate ion adsorption; but steric factors determining the ease of fit in the film may be decisive. Data on interatomic spacings suggest that, provided there are two adjacent vacancies in the lattice, an SO_4^{2-} ion fits readily into the oxide lattice because the distance between oxygen ions in Al_2O_3 is identical to that between oxygen atoms in the SO_4^{2-} ion. It also appears that the ease of fit of the SO_4^{2-} ion is due to the fact that it fits equally well, whichever pair of oxygen atoms reaches the surface first, i.e., it is symmetrical. With oxalate ion, only the end pair of oxygen atoms fits into the oxide lattice. Since the oxide film at the oxide-electrolyte interface is visualized as a 2-dimensional lattice, a reduction of half the number of available ions for inclusion into it makes it possible that the incorporation of oxalate is $(1/2)^2$, i.e., one-fourth of the SO_4^{2-} ion. This deduction augurs well with the evidence of 3 % ion introduction in oxalic acid as compared to 15 % in sulphuric acid.

Salt doping is another method used for ion inclusion [49-56]; see Table 1. The LiCl salt is uniformly dispersed in dilute concentrations of 1-3% by volume on the substrate of a thin film sensor, and the salt is usually embedded in a thin coating of binder material.

Dynamic behavior of the sensor is determined by moisture adsorption through top electrode and circumferentially, and diffusion coefficient of water vapor in the dielectric. Provision of an integrated heater as a thermal resetting device is also used for fast recovery after high humidity exposure. Thus important tools are surface conductivity control by ionic doping, layout of geometry of the top electrode and overall sensor structural design. Which parameter is to be chosen depends on the requirements of the situation.

8. Conclusions and Outlook

Humidity-sensor models are reviewed, selected models are elaborated and their contribution towards designing humidity sensors of given specifications is highlighted, notably in fabricating sensors for assigned humidity ranges and providing quick response; also in controlling the sensitivity, linearity and hysteresis in characteristics. The models advance the level of understanding on the processes governing the operation of the sensor and establishing the design guidelines for fabricating sensors of desired response characteristics. Notwithstanding the above success, rummaging through the models, it is observed that although several facets of humidity sensor behavior have been understood, formulation of a complete theory faithfully representing it in entirety and encompassing all its salient features, continues to elude solution and remains a formidable research problem confronting scientists.

Humidity sensors offer many fascinating and rewarding areas for fundamental study and commercial exploitation. A quantitative correlation of the exact amount of ionic dopant with the humidity sensitivity of the device is an interesting problem for further investigation. Another topic is the development of techniques for decelerating the sensor ageing and detailed studies of the rate of calibration drift.

Table 1. Influence of salt doping on humidity sensor characteristics, as reported by various workers.

Sl. No.	Dielectric material	Doping salt (s)	Relative humidity range studied	Effects noticed	Reference
1.	$BaTiO_3$	3-5 wt% Na_2CO_3 or K_2CO_3	10-98 %	Resistance of the humidity sensor is decreased to the range 1-10^3 kΩ. Addition of NaH_2PO_4 reduced the humidity hysteresis.	[50]
2.	$0.5ZrO_2$–$0.5TiO_2$ ceramic	2 and 5 % mol $LiOH.H_2O$	20-95 %	Li^+ ions increased the sensitivity by an order of two, and also improved the linearity.	[51]
3.	Poly(methyl methacrylate) (PMMA)	KOH (0.6%, w/w) and K_2CO3 (0.6%, w/w)	30–90 %	Optimal in both sensitivity and linearity.	[52]
4.	UV sensitive epoxy resin	Deliquescent salt of magnesium chloride ($MgCl_2$)	> 33 %	Sensitivity of the porous structure doped with 1.2 wt% of $MgCl_2$ was enhanced over 365-fold greater than the sensor fabricated with the same material without ion doping.	[53]
5.	TiO_2-20 wt.% SnO_2	0.5 wt.% of La_2O_3/Ce_2O_3	15–95 %	Impedance decreased from 10^9 Ω to 10^4 Ω or less.	[54]
6.	MEBA-co-KH570 Copolymer	LiCl, $CaCl_2$ or $FeCl_3$	33 %-95 %	Sensors exhibited high sensitivities and good linearities. At an optimal doping concentration (1×10^{-2} mol/L) of LiCl, the sensor gave the best sensitivity and the shortest desorption time (20 s)	[55]
7.	TiO_2 ceramics	LiCl and KCl	10-70 %	Sensitivity improvement; a variation in resistance by two orders of magnitude over a range of humidity of 25-65 % RH with good reversibility.	[56]

Acknowledgements

The author wishes thank the Director, CSIR-CEERI, Pilani for encouragement and guidance.

Nomenclature

a: radius of cylinder
BET theory: Brunauer-Emmett-Teller Theory
C_0: Capacitance of a mixed (air+water +alumina) dielectric
C_B: Capacitance of the pore base
$C_{\mathbf{Norm,Film}}(t)$: Normalized capacitance with respect to steady-state capacitance, as a function of time
D: Diffusion coefficient or diffusivity of moisture
d:Thickness of the dielectric film of the capacitor/diffusing medium
$d\varepsilon'/d\eta$: Rate of change of real part of complex permittivity with humidity
h :Height of the cylindrical film
$h_Q(t)$: Humidity impulse as a function of time (t)
J, J_1, J_2: Current densities of anodization
J_0 :Bessel function of the first kind of zero order
k_n's : Roots of an equation
l: Length of the film
n: An integer
p: Interline spacing
q: Number of lines
r: Width of the line
R_0: Resistance of a mixed (air+water +alumina) dielectric; DC leakage resistance
R_S: Pore side resistance
R_B: Resistance of the pore base
t: Time
$t_{\mathbf{Film}}$: Response time of film
t_{Cyl}: Response time of cylinder
T: Temperature in Kelvin scale

α_n's: Roots of an equation
γ: Volume fraction of water present in the dielectric at a given humidity
Γ: A parameter connected with shape parameter λ of the pores
ε: Complex dielectric constant; effective relative permittivity
ε_0: Permittivity of free space
ε_a: Relative permittivity of air
ε_m: Relative permittivity of (air+solid) mixed dielectric
ε': Real component of complex permittivity
ε_∞ : Optical dielectric constant
ε_p: Dielectric constant of sensing film without water
ε_s: Relative permittivity of sensing film
ε_w: Dielectric constant of water
η : Humidity
λ : A shape parameter of the pores
ω: Angular frequency
ρ : Charge density
ξ, ξ': Constants
τ: Time constant

References

[1]. C. T. Okada (Ed.), Humidity Sensors: Types, Nanomaterials and Environmental Monitoring, *Nova Science Pub Inc.,* 2011.

[2]. Y. J. Liu, J. Shi, F. Zhang, H. Liang, J. Xu, A. Lakhtakia, S. J. Fonash and T. J. Huang, High-speed Optical Humidity Sensors Based on Chiral Sculptured Thin Films, *Sensors and Actuators B: Chemical*, Vol. 156, Issue 2, 2011, pp. 593– 598.

[3]. A. Buvailoa, Y. Xing, J. Hines, and E. Borguet, Thin Polymer Film Based Rapid Surface Acoustic Wave Humidity Sensors, *Sensors and Actuators B: Chemical*, Vol. 156, Issue 1, 2011, pp. 444–449.

[4]. M.-Z. Yang, C.-L. Dai and W.-Y. Li, Fabrication and Characterization of Polyaniline/PVA Humidity Microsensors, *Sensors*, Vol. 11, 2011, pp. 8143-8151.

[5]. M. G. Kovac, D. Chleck and P. Goodman, A New Moisture Sensor for *In Situ* Monitoring of Sealed Packages, *Solid State Technology*, Vol. 21, 1978, pp. 35-39.

[6]. S. Hasegawa, Performance Characteristics of a Thin Film Aluminium Oxide Humidity Sensor, in *30th IEEE Electronic Components Conference*, San Francisco, CA, April 28-30, 1980, pp. 386-391.

[7]. R. K. Nahar and V. K. Khanna, A Study of Capacitance and Resistance Characteristics of an Al_2O_3 Humidity Sensor, *International Journal of Electronics*, Vol. 52, 1982, pp. 557-567.

[8]. K. Sugaya, New Thick Film, Humidity Sensor, in *Proc. International Microelectronics Conference*, ISHM, Tokyo, May 24-26, 1982, pp. 157-162.

[9]. S. Iwanaga, N. Sato and A. Ikegami, Characteristics and Reliability of Thick Film Humidity sensor, *Proc. International Microelectronics Conference*, ISHM, Tokyo, May 24-26, 1982, pp. 149-156.

[10]. W. Smetana and W. Wiedermann, Experimental Characterization of Thick Film Dielectrics for Humidity-Sensor Application, in *Proc. 4th European Hybrid Microelectronics Conference*, ISHM, Copenhagen, 1983, pp. 203-210.

[11]. G. Delapierre, H. Grange, B. Chambaz and L. Destannes, Polymer-based Capacitive Humidity Sensor: Characteristics and Experimental Results, *Sensors and Actuators*, Vol. 4, 1983, pp. 97-104.

[12]. Y. Sakai and Y. Sadaoka, Humidity Sensors Using Sulphonated Microporous Polyethylene Films, *Denki Kagaku* (Japan), Vol. 53, 1985, pp. 150-151.

[13]. S. Tsuchitani, T. Sugawara, N. Kinjo and S. Ohara, Humidity Sensor Using Ionic Copolymer, in *3rd Int. IEEE Conference on Solid-State Sensors and Actuators*, Philadelphia, PA, USA, June 11-14, 1985, pp. 210-212.

[14]. N. Ichinose, Ceramic Materials Herald the Future of Sensors, *J. Electron. Eng*., Vol. 23, 1986, pp. 93-95.

[15]. G. M. O' Halloran, P. M. Sarro, J. Groeneweg, P. J. Trimp and P. J. French, A Bulk Micromachined Humidity Sensor Based on Porous Silicon, in *International Conference on Solid State Sensors and Actuators, TRANSDUCERS '97*, 16 -19 Jun 1997, Chicago, IL, USA, Vol. 1, pp. 563–566.

[16]. T.-Y. Yang, J. J. Huang, C.-Y. Liu and H.-Y. Wang, A CMOS-MEMS Humidity Sensor, in *International Conference on Circuits, System and Simulation*. IPCSIT, Vol. 7, 2011, pp. 212-217.

[17]. Y. Zhang, K. Yu, D. Jiang, Z. Zhu, H. Geng and L. Luo, Zinc Oxide Nanorod and Nanowire for Humidity Sensor, *Applied Surface Science*, Vol. 242, Issues 1-2, 2005, pp. 212-217.

[18]. Y. Zhang, K. Yu, S. Ouyang, L. Luo, H. Hu, Q. Zhang and Z. Zhu, Detection of Humidity Based on Quartz Crystal Microbalance Coated with ZnO Nanostructure Films, *Physica B: Condensed Matter*, Vol. 368, Issues 1-4, 2005, pp. 94-99.

[19]. X.-H. Wang, Y.-F. Ding, J. Zhang, Z.-Q. Zhu, S.-Z. You, S.-Q. Chen and J. Zhu, Humidity Sensitive Properties of ZnO Nanotetrapods Investigated by a Quartz Crystal Microbalance, *Sensors and Actuators B: Chemical*, Vol. 115, Issue 1, 2006, pp. 421-427.

[20]. A. I. Buvailo, Y. Xing, J. Hines, N. Dollahon and E. Borguet, TiO_2/LiCl-based Nanostructured Thin Film for Humidity Sensor Applications, *ACS Appl. Mater. Interfaces*, Vol. 3, Issue 2, 2011, pp. 528–533.

[21]. C. L. Cao, C. G. Hu, L. Fang, S. X. Wang, Y. S. Tian and C. Y. Pan, Humidity Sensor Based on Multi-Walled Carbon Nanotube Thin Films, *Journal of Nanomaterials*, Article ID 707303, 2011, 5 pages.

[22]. F. Asbacher and A. C. Jason, Some Electrical Effects of the Adsorption of Water by Anodised Aluminium, *Nature*, Vol. 171, 1953, pp. 177-178.

[23]. A. C. Jason and J. L. Wood, Some Electrical Effects of the Adsorption of Water Vapour by Anodized Aluminium, *Proc. Phys. Soc.* B, Vol. 68, 1955, pp. 1105-1116.

[24]. C. J. L. Booker and J. L. Wood, Further Electrical Effects of the Adsorption of Water Vapour by Anodised Aluminium, *Proc. Phys. Soc. B*, Vol. 76, 1960, pp. 721-731.

[25]. A. E. Falk, B. M. Lacquet and P. L. Swart, Determination of Equivalent Circuit Parameters of Porous Dielectric Humidity Sensors, *Electronics Letters*, Vol. 28, Issue 2, 1992, pp. 166-167.

[26]. V. K. Khanna and R. K. Nahar, Effect of Moisture on the Dielectric Properties of Porous Alumina Films, *Sensors and Actuators*, Vol. 5, 1984, pp. 187-198.

[27]. V. K. Khanna and R. K. Nahar, Carrier-Transfer Mechanisms and Al_2O_3 Sensors for Low and High Humidities, *Journal of Physics D: Applied Physics*, Vol. 19, 1986, pp. L141-L145.

[28]. V. K. Khanna and R. K. Nahar, Surface Conduction Mechanisms and the Electrical Properties of Al_2O_3 Humidity Sensor, *Applied Surface Science*, Vol. 28, 1987, pp. 247-264.

[29]. V. K. Khanna, Development, Characterization and Modeling of the Porous Alumina Humidity Sensor (Ph. D Thesis), *Kurukshetra University,* Kurukshetra, 1987.

[30]. R. K. Nahar, V. K. Khanna and W. S. Khokle, On the Origin of the Humidity-sensitive Electrical Properties of Porous Aluminium Oxide, *Journal of Physics D: Applied Physics*, Vol. 17, 1984, pp. 2087-2095.

[31]. R. K. Nahar and V. K. Khanna, Ionic Doping and Inversion of the Characteristic of Thin Film Porous Al_2O_3 Humidity Sensor, *Sensors and Actuators B: Chemical*, Vol. 46, Issue 1, 1998, pp. 35-41.

[32]. R. K. Nahar, Study of the Performance Degradation of Thin Film Aluminum Oxide Sensor at High Humidity, *Sensors and Actuat*ors *B: Chemical*, Vol. 63, Issues 1-2, 2000, pp. 49–54.

[33]. R. K. Nahar, Physical Understanding of Moisture Induced Degradation of Nanoporous Aluminum Oxide Thin Films, *J. Vac. Sci. Technol. B*, Vol. 20, 2002, p. 382 (4 pages).

[34]. S. Brunauer, P. H. Emmette and E. Teller, Adsorption of Gases in Multimolecular Layers, *Journal of the American Chemical Society*, Vol. 60, 1938, pp. 309-319.

[35]. S. Brunauer, L. S. Demming, W. E. Deming and E. Teller, On a Theory of Van der Waals Adsorption of Gases, *J. Am. Chem. Soc*., Vol. 62, 1940, pp. 1723-1732.

[36]. L. R. Fisher, R. A. Gamble and J. Middlehurst, The Kelvin Equation and the Capillary Condensation of Water, *Nature*, Vol. 290, 1981, pp. 575-576.

[37]. R. W. Sillars, The Properties of a Dielectric Containing Semiconducting Particles of Various Shapes*, J. Inst. Elec. Eng*., Vol. 80, 1937, pp. 378-394.

[38]. B. Naiman, The Debye-Huckel Theory and its Application in the Teaching of Quantitative Analysis, *J. Chem. Educ.,* Vol. 26, No. 5, 1949, p. 280.

[39]. U. Kang and K. D. Wise, A High-speed Capacitive Humidity Sensor with On-chip Thermal Reset, *IEEE Transactions on Electron Devices*, Vol. 47, No. 4, 2000, pp. 702-710.

[40]. A. Tetelin and C. Pellet, Accurate Model of the Dynamic Response of a Capacitive Humidity Sensor, in *Proc. 2nd IEEE Sensors Conf.,* Vol. 1, Toronto, ON, Canada, Oct. 21–24, 2003, pp. 378–383.

[41]. A. Tetelin, V. Pouget, J.-L. Lachaud and C. Pellet, Dynamic Behavior of a Chemical Sensor for Humidity Level Measurement in Human Breath, *IEEE Transactions on Instrumentation and Measurement*, Vol. 53, No. 4, 2004, pp. 1262-1267.

[42]. A. Tetelin and C. Pellet, Modeling and Optimization of a Fast Response Capacitive Humidity Sensor, *IEEE Sensors Journal*, Vol. 6, No. 3, 2006, pp. 714-720.

[43]. L. Chandran, H. Baltes and J. Korvink, Three-dimensional Modeling of Capacitive Humidity Sensors, *Sensors and Actuators A: Physical*, Vol. 25, Issues 1-3, 1990, pp. 243-247.

[44]. A. K. Sen and J. Darabi*,* Modeling and Optimization of a Microscale Capacitive Humidity Sensor for HVAC Applications, *IEEE Sensors Journal*, Vol. 8, No. 4, 2008, pp. 333-340.

[45]. P. J. Schubert and J. H. Nevin, Polyimide-Based Capacitive Humidity Sensor, *IEEE Trans. Electron Devices*, Vol. ED-32, No. 7, 1985, pp. 1220–1223.

[46]. R. Fenner and E. Zdankiewicz, Micromachined Water Vapor Sensors: A Review of Sensing Technologies, *IEEE Sensors J.,* Vol. 1, No. 4, 2001, pp. 309–317.
[47]. H. Shibata, M. Ito, M. Asakursa and K. Waltanabe, A Digital Hygrometer Using a Polyimide Film Relative Humidity Sensor, *IEEE Trans. Instrum. Meas.,* Vol. 45, No. 2, 1996, pp. 564–569.
[48]. G. C. Wood, in Oxides and Oxide Films, J. W. Diggle (Ed.), Vol. 2, *Dekker,* New York, 1973, pp. 167-279.
[49]. Y. Sadaoka, H. Aono, Y. Sakai, S. Nakayama and H. Kurosima, Humidity Sensor Using KH_2PO_4-doped Porous Ferroelectrics, *J. Materials Science Letters*, Vol. 9, 1986, pp. 923-924.
[50]. J. Wang, B. Xu, G. Liu, Y. Liu, F. Wu, X. Li and M. Zhao, Influence of Doping on Humidity Sensing Properties of Nanocrystalline $BaTiO_3$, *Journal of Materials Science Letters*, Vol. 17, 1998, pp. 857-859.
[51]. M. K. Jain, M. C. Bhatnagar, and G. L. Sharma, Effect of Li^+ Doping on ZrO_2–TiO_2 Humidity Sensor, *Sensors and Actuators B: Chemical*, Vol. 55, Issues 2-3, 1999, pp. 180–185.
[52]. G. Casalbore-Miceli, M. Yang, Y. Li, N. Camaioni, A. Martelli and A. Zanelli, Effect of the Doping Level on the Conductance of Polymer–salts Complexes in the Presence of Humidity, *Sensors and Actuators B: Chemical*, Vol. 97, Issues 2-3, 2004, pp. 362-368.
[53]. C.-H. Chen, C.-W. Hung and C.-H. Lin, *In-situ* Formation of an Ion-doped Porous Structure for High Sensitive Humidity Sensing Utilizing Low-Cost UV Sensitive Glue, in *IEEE Transducers 2009*, Denver, CO, USA, June 21-25, 2009, pp. 1694-1697.
[54]. L. Hongxia, S. Zhiming and L. Hongwei, Humidity Sensing Properties of La^{3+}/Ce^{3+}-Doped TiO_2-20 wt. % SnO_2 Thin Films Derived from Sol-Gel Method, *Journal of Rare Earths*, Vol. 28, No. 1, 2010, pp. 123-127.
[55]. H. Lin, W. Yu-Cheng, S. Ai-Hua, L. Yong and C. Ping, Humidity-Sensitive Properties of Salt-doped MEBA-*co*-KH570 Copolymer, *Chinese Journal of Applied Chemistry*, Vol. 27, Issue 1, 2010, pp. 43-47.
[56]. A. I. Buvailo, Y. Xing, J. Hines, N. Dollahon, and E. Borguet, TiO_2/LiCl-Based Nanostructured Thin Film for Humidity Sensor Applications, *Appl. Mater. Interfaces*, Vol. 3, 2011, pp. 528–533.
